DOI: http://dx.doi.org/10.32571/ijct.755732 **E-ISSN: 2602-277X**

International Journal of Chemistry and Technology

http://dergipark.org.tr/ijct

Research Article

Synthesis of magnetic Fe_3O_4/AC nanoparticles and its application for the removal of gas-phase toluene by adsorption process

Sinan KUTLUAY[1,*], Mehmet Şakir ECE[2], Ömer ŞAHİN[1]

[1]*Department of Chemical Engineering, Faculty of Engineering, Siirt University, Siirt 56100, Turkey*

[2]*Vocational High School of Health Services, Mardin Artuklu University, Mardin 47100, Turkey*

Received: 21 June 2020; Revised: 04 September 2020; Accepted: 05 September 2020

*Corresponding author e-mail: sinankutluay@siirt.edu.tr

Citation: Kutluay, S.; Ece, M. Ş.; Şahin, Ö. *Int. J. Chem. Technol.* **2020**, 4 (2), 146-155.

ABSTRACT

In this study, we present the first application of magnetic Fe_3O_4 functionalized with activated carbon (Fe_3O_4/AC) as nano-adsorbent for the removal of gas-phase toluene by adsorption process. Magnetic Fe_3O_4/AC was synthesized via co-precipitation method within the framework of nanotechnology principles. Then, the effects of process conditions such as contact time, initial toluene concentration, and temperature on the adsorption capacity of toluene by the magnetic Fe_3O_4/AC were investigated using the response surface methodology (RSM). The obtained magnetic Fe_3O_4/AC was characterized using scanning electron microscopy (SEM), fourier transform infrared spectroscopy (FTIR) and thermogravimetric (TG) analysis. The maximum adsorption capacity of the magnetic Fe_3O_4/AC for the adsorption of the toluene was determined as 312.99 mg g^{-1} under optimal process conditions such as 59.48 min contact time, 17.21 mg l^{-1} initial toluene concentration, and 26.01°C temperature. The adsorption by the magnetic Fe3O4/AC indicated the best fit with the Langmuir isotherm model, and obeyed the pseudo-second-order (PSO) kinetic model. This study indicated that magnetic Fe_3O_4/AC could be applied as an adsorbent for the removal of gas-phase toluene.

Keywords: **N**anotechnology, magnetic nano-adsorbents, response surface methodology, adsorption, toluene.

Manyetik Fe_3O_4/aktif karbon nanoparçacıklarının sentezlenmesi ve adsorpsiyon prosesi ile gaz-fazındaki toluenin giderilmesi için uygulanması

ÖZ

Bu çalışmada, gaz-fazı toluenin adsorpsiyon prosesi ile giderilmesi için nano-adsorbent olarak aktif karbon ile fonksiyonelleştirilmiş manyetik Fe_3O_4 (Fe_3O_4/AC)'nin ilk uygulamasını sunuyoruz. Manyetik Fe_3O_4/AC, nanoteknoloji prensipleri çerçevesinde birlikte çöktürme yöntemi ile sentezlendi. Daha sonra, temas süresi, başlangıç toluen konsantrasyonu ve sıcaklık gibi proses koşullarının toluenin manyetik Fe_3O_4/AC ile adsorpsiyonu üzerindeki etkileri yanıt yüzeyi yöntemi (RSM) kullanılarak incelendi. Elde edilen manyetik Fe_3O_4/AC, taramalı elektron mikroskopisi (SEM), fourier dönüşümü kızılötesi spektroskopisi (FTIR) ve termogravimetrik (TG) analiz kullanılarak karakterize edildi. Toluenin adsorpsiyonu için manyetik Fe_3O_4/AC' nin maksimum adsorpsiyon kapasitesi, 59,48 dakika temas süresi, 17,21 mg l^{-1} başlangıç toluen konsantrasyonu ve 26,01°C sıcaklıktaki proses koşulları altında 312,99 mg g^{-1} olarak belirlendi. Manyetik Fe3O4/AC tarafından adsorpsiyon, Langmuir izoterm modeli ile en iyi uyumu gösterdi ve sözde ikinci dereceden (PSO) kinetik modele uydu. Bu çalışma, manyetik Fe_3O_4/AC'nin, gaz-fazı toluenin giderilmesi için bir adsorbent olarak uygulanabileceğini gösterdi.

Anahtar Kelimeler: Nanoteknoloji, manyetik nano-adsorbentler, yanıt yüzey metodu, adsorpsiyon, toluen.

1. INTRODUCTION

Volatile organic compounds (VOCs), which cause even adverse health problems such as cancer, are a major component of atmospheric pollutants. VOCs are important air pollutants because of such detrimental effects as allergic reactions, nausea, throat irritation, nose, eye and headache. Besides, they cause dangerous environmental problems such as photochemical smog, suspended particulate matter, stratospheric ozone depletion and global warming. Among VOCs, toluene pollutes the air because of tanning processes, some

DOI: http://dx.doi.org/10.32571/ijct.755732 **E-ISSN: 2602-277X**

printing processes, adhesives, paints, wastewater, industrial activities and automobiles. Also, toluene is a chemical with high motility, toxicity, carcinogenicity, and teratogenicity. The accumulation of toluene in the air, food chain and groundwater endangers the security of both people and the ecosystem. World Health Organization (WHO) has declared in 1986 that because of its chronic effect on human health, the toluene concentration should not exceed 0.2–0.4 mg l^{-1}. Hence, toluene needs to be eliminated in order to preserve both human health and the environment.[1-4]

Industrial sectors considerably intrude the gas rates in the air. Adverse effects on air quality affect health negatively. It is a vital requirement to decrease the infiltration of poisonous gases in the atmosphere and to develop reduction strategies. Therefore, pollutant removal methods have become indispensable.There are various techniques have been widely used for the removal of VOC pollutants.[5-6] Among these techniques, the adsorption is one of the least harmful process as well as high yield, cheap, simplicity, and renewable properties.[7-9] In this sense, nanotechnology offers more unusual and impressive solutions than other traditional methods in adsorption technology, as in all other fields. Fe_3O_4 is a common material widely examined in nanotechnological researches. It has attracted considerable attention because of its magnetic properties such as biocompatibility, low-toxicity, low cost and high surface area. It efficiently solves different analytical and industrial problems. Fe_3O_4 presents high surface areas for adsorption, helps recovery due to its magnetic property, and most importantly, it has low toxicity. It is a green and secure option for environmental improvement because of its unique properties such as size, surface area, absorptivity, electronic and catalytic properties.[10]

This study focused on the application of the toluene adsorption by the magnetic Fe_3O_4/AC as nano-adsorbent. In this context, the effects of process conditions such as contact time, initial toluene concentration, and temperature on the adsorption capacity of toluene were investigated. The obtained magnetic Fe_3O_4/AC was characterized using scanning electron microscopy (SEM), fourier transform infrared spectroscopy (FTIR) and thermogravimetric (TG) analysis. Also, the kinetics process of toluene adsorption was evaluated using kinetic models. Equilibrium adsorption data of toluene were defined by isotherm models.

2. MATERIALS AND METHODS

2.1. Materials

Iron (III) chloride hexahydrate ($FeCl_3.6H_2O$) and activated carbon (AC, Z29CO045) were supplied from Merck Chemical. Iron (II) chloride tetrahydrate ($FeCl_2.4H_20$) was bought from ALFA AESAR Chemical Company. Ethanol (CH_3CH_2OH) from Sigma-Aldrıch Chemical Companies. Ammonia (NH_3) from VWR Chemicals. All chemicals and solvents and toluene (99.0%) used as adsorbate provided from Sigma Aldrich, and they have analytical purity.

2.2. Synthesis of the magnetic Fe_3O_4/AC

The magnetic Fe_3O_4/AC was synthesized applying the co-precipitation method, which is a straight forward and convenient approach. In magnetic Fe_3O_4/AC synthesis, a mixture of 4 mmol $FeCl_3.6H_2O$ and 2 mmol $FeCl_2.4H_2O$ was distributed stoichiometrically in a mixture of 50 ml deionized-distilled water in a way that Fe^{+2} / Fe^{+3} ratio would be 1/2, and AC was added in the mixture with an amount that the mass ratio of (Fe^{+2}+Fe^{+3})/(AC) would be 4/1. It was sonicated for 10 min. 10 ml NH_3 solution was added drop by drop to obtain co-precipitation. Amalgamating was continued under argon at 50°C for 30 min. The Fe_3O_4/AC obtained as a product was isolated from the medium by magnetic separation. Then Fe_3O_4/AC washed several times with deionized-distilled water and ethanol. Immediately after, the Fe_3O_4/AC was dried in a vacuum oven for 20 h at 50°C.[11] The synthesis of magnetic Fe_3O_4/AC is displayed schematically in Figure 1.

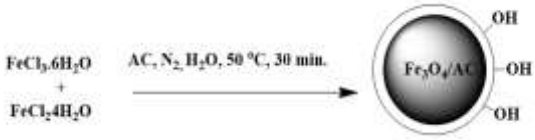

Figure 1. Schematic representation of the synthesis of magnetic Fe_3O_4/AC.

2.3. Gas-phase adsorption of toluene

Detailed information for the dynamic adsorption of toluene by the magnetic Fe_3O_4/AC was presented in the previously published procedure.[12] The capacity of the magnetic Fe_3O_4/AC to adsorb toluene was estimated at atmospheric pressure. The flow rate of the gas (N_2) employed as the carrier during the adsorption process was 100 ml min^{-1}. The optimum amount of magnetic Fe_3O_4/AC was 80 mg.

The adsorption capacity was estimated with Eq. (1) presented below:[13]

$$q = \frac{F}{m}\int_0^t (C_{in} - C_{eff})dt \quad (1)$$

In this situation, m (g) is the amount of the magnetic

DOI: http://dx.doi.org/10.32571/ijct.755732 **E-ISSN: 2602-277X**

Fe_3O_4/AC. F (l min^{-1}) is the gas flow rate, t (min) is the contact time. C_{in} and C_{eff} (mg l^{-1}) are the initial and out toluene concentrations, respectively, q (mg g^{-1}) is the adsorption capacity.

2.4. Characterization

The surface characteristics of the synthesized magnetic Fe_3O_4/AC were recorded with an FTIR (Bruker Vertex 70) spectrometer in the range of 4000-400 cm^{-1}. The magnetic Fe_3O_4/AC surface morphology was characterized by SEM (Zeiss EVO 50 Model) analysis. TG thermogram accomplished with Shimadzu DTG-60 was conducted to define the formation of the magnetic Fe_3O_4/AC and the number of functional groups appended to the surface. Mathematical modeling, statistical analysis, and optimization studies for experimental data were conducted by employing Design Expert 12.0.8.0 Software (Free Trial Version).

3. RESULTS AND DISCUSSION

3.1. Characterization of the magnetic Fe_3O_4/AC

Characterization of the magnetic Fe_3O_4/AC was conducted by FTIR, TG, and SEM analysis. SEM images, FTIR spectra, and TG thermogram of the synthesized magnetic Fe_3O_4/AC were presented in Figures 2-4, respectively.

3.1.1. SEM analysis

The SEM microstructure image of AC was presented in Figure 2a. As observed in Figure 2a, AC has surface roughness. Various sizes of heterogeneous pores and cavities are clearly noticeable on the AC surface. The SEM microstructure image of the magnetic Fe_3O_4/AC is presented in Figure 2b. When the magnetic Fe_3O_4/AC microstructure image was analyzed, it was observed that the general pore formation was rough and spongy. It was understood that the intrusions, protrusions, and roughness increased the surface area in the magnetic Fe_3O_4/AC microstructure compared to the microstructure of AC.

3.1.2. FT-IR analysis

FTIR spectrum of the magnetic Fe_3O_4/AC is presented in Figure 3. As observed in Figure 3, the peak at 550 cm-1 which is the characteristic for Fe3O4, indicates the presence of Fe-O bonds.. Still, the peaks at 3448 cm^{-1} and 1404 cm^{-1} indicate the stress and vibration peaks of O-H, respectively. The peak at 1656 cm^{-1} shows the vibration peak of the C-C bond, and the peak at 1118 cm^{-1} shows the vibration peak of the C-O bond.

The determined peak values are in accordance with the values presented in the literature.[14]

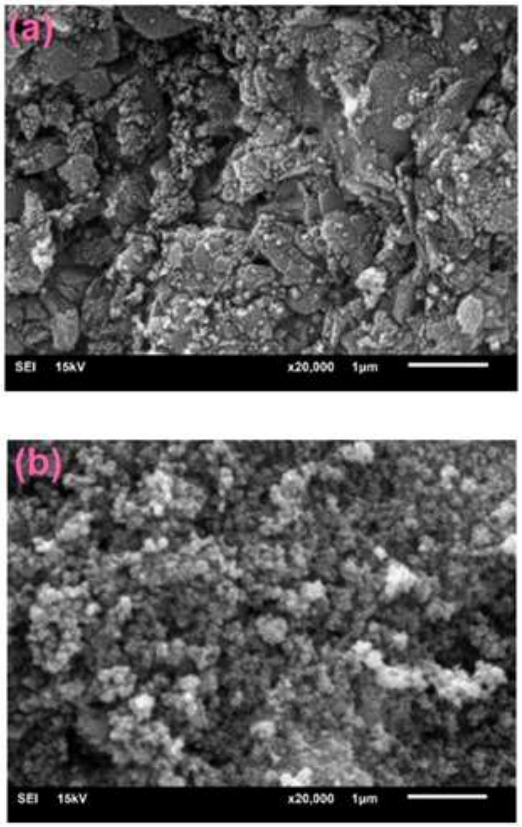

Figure 2. SEM images of a) AC, b) Magnetic Fe_3O_4/AC.

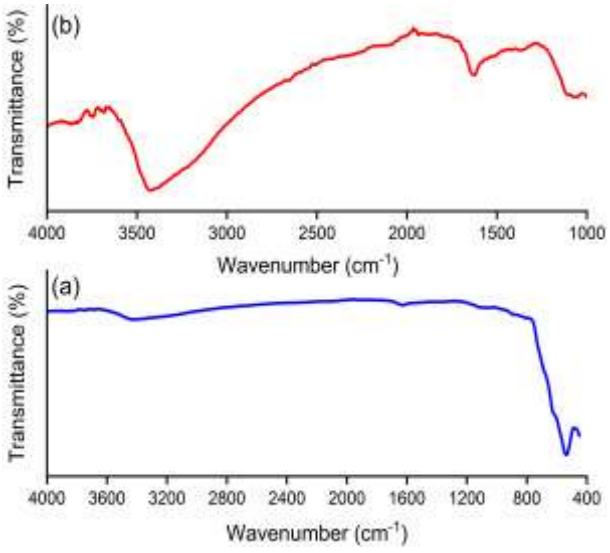

Figure 3. FT-IR spectra of a) the magnetic Fe_3O_4/AC, b) Fe_3O_4/AC.

DOI: http://dx.doi.org/10.32571/ijct.755732 E-ISSN: 2602-277X

3.1.3. TG analysis

TG analysis is a technique, as a function of temperature under a controlled atmosphere, applied to determine the weight changes of a sample. The thermal stability of a sample can also be observed practicing TG analysis. The TG curve of the magnetic Fe_3O_4/AC is presented in Figure 4.

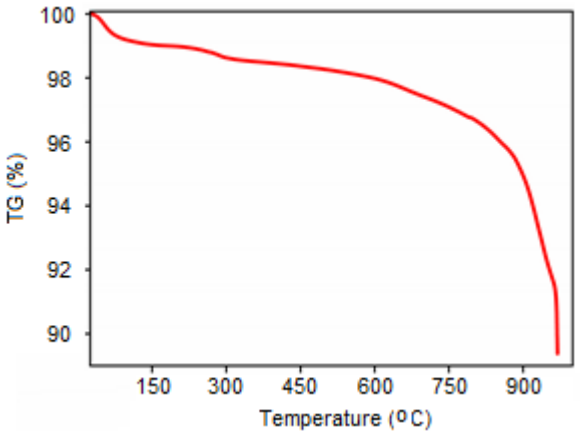

Figure 4. TG curve of the magnetic Fe_3O_4/AC.

As seen in Figure 4, the percentage of magnetic Fe_3O_4/AC's TG temperature-weight loss graph is approximately 10.6%. This percentage summarized the magnetic Fe_3O_4/AC residue after the decomposition stage in the thermogram, with a limited reduction in thermal stability. The loss between 25-540°C is a consequence of volatile organic compounds and water loss remaining in the sample. The loss between 500-970°C is related to low decomposition.

3.2. Experimental design, statistical analysis and optimization for the adsorption of toluene

In this study, RSM, which is an experimental method for the development, improvement, and optimization of the design process, was applied to determine the importance of the potential interactions of the functioning parameters. The approach of RSM-based central composite design (CCD) was employed to perform statistical analyses and obtain the regression model. Statistically significant model parameters were determined by using the variance analysis (ANOVA). For the study, the effects of parameters such as contact time (A), initial toluene concentration (B), and temperature (C) were analyzed. The values of the design points of the parameters are presented in Table 1. Table 2 show the parameter values for 17 experiments in the CCD experimental design and the capacities of the magnetic Fe_3O_4/AC for the toluene adsorption obtained according to the experimental and predicted model.

The adsorption capacity of the magnetic Fe_3O_4/AC for the toluene adsorption was statistically analyzed employing ANOVA, and the results obtained are presented in Table 3. ANOVA shows which factor is most significant in an experimental design. It also defines the relationship between the factors studied and provides information about whether the results of the experiment are significant.[15] The validity and reliability of the proposed model are assessed according to p-value, F-value, correlation coefficients (R^2), and adeq precision results. In other words, the proposed model was suitable in the situation indicating $p < 0.05$, $F > 4$, $R^2 > 0.95$, and adeq precision > 4. As seen in Table 3, when the ANOVA results obtained for the magnetic Fe_3O_4/AC capacity for the toluene adsorption were analyzed, it was observed that A, B, and C were important model terms ($p < 0.05$). The high value of the correlation coefficient (R^2 = 0.98) for the adsorption capacity signified evidence of a good fit between the experimental data and the model. The R^2 value of 98% means that 99% of the total variation for the adsorption capacity was represented by variable factors.[16] Besides, the F-value of 49.96 and adeq precision results of 22.44 indicated that the proposed model well defined experimental data. Moreover, the fact that the experimental and model adsorption capacity values presented in Table 2 were very close to each other verified the validity and reliability of the proposed model.

The contour (2D) plots of the interaction effects of the two factors on the capacity of the magnetic Fe_3O_4/AC for the toluene adsorption are presented in Figure 5. As seen in Figure 5a, adsorption capacity increased with increasing contact time. The number of active sites on the nano-adsorbent surface can be regarded as the reason for this situation.[17] It was seen that the adsorption capacity did not significantly change with increasing initial toluene concentration. Figure 5b presents the relationship between contact time and temperature. The highest adsorption capacity was seen at a high contact time and low temperature. Notably, the amount of temperature had an essential effect on the adsorption capacity. ANOVA results supported this situation. When the surface plot for the initial toluene concentration versus temperature (Figure 5c) was considered, it was evident that the initial toluene concentration did not have a meaningful effect on the adsorption capacity, while the highest adsorption capacity was seen when the temperature was close to approximately 25°C.

DOI: http://dx.doi.org/10.32571/ijct.755732 **E-ISSN: 2602-277X**

Table 1. Operating factors and properties in experimental design

Factors	Operating ranges and values				
	-α (-1.682)	**-1**	**0**	**+1**	**+α (+1.682)**
A: Contact time (min)	6.36	20	40	60	73.64
B: Concentration (mg l^{-1})	6.59	10	15	20	23.41
C: Temperature (°C)	19.88	25	32.5	40	45.11

Table 2. Experimental design and CCD approach results for the adsorption of toluene by the magnetic Fe_3O_4/AC

Run	A	B	C	Actual	Predicted
	Contact time (min)	**Concentration (mg l^{-1})**	**Temperature (°C)**	**Adsorption capacity (mg g^{-1})**	**Adsorption capacity (mg g^{-1})**
1	60	20	25	313	310
2	20	20	40	174	177
3	40	15	45.11	191	185
4	60	10	25	252	247
5	20	10	40	71	68
6	40	15	32.5	264	260
7	60	10	40	238	232
8	20	10	25	132	130
9	6.36	15	32.5	86	82
10	40	15	32.5	262	255
11	40	15	32.5	263	269
12	20	20	25	212	209
13	40	6.59	32.5	134	129
14	40	15	19.88	295	290
15	73.64	15	32.5	276	271
16	40	23.41	32.5	266	260
17	60	20	40	239	245

Process conditions were optimized to define the maximum adsorption capacity value for toluene. In the optimization process, the values such as the contact time, initial toluene concentration, and temperature were analyzed in the operating range. Optimum adsorption conditions were defined applying the desirability program for maximum adsorption capacity of toluene by the magnetic Fe_3O_4/AC, and the optimum results obtained are presented in Figure 6. The maximum adsorption capacity of the magnetic Fe_3O_4/AC for the toluene adsorption was determined as 312.99 mg g^{-1} under optimal process conditions such as 59.48 min contact time, 17.21 mg l^{-1} initial toluene concentration, and 26.01°C temperature.

DOI: http://dx.doi.org/10.32571/ijct.755732 **E-ISSN: 2602-277X**

Table 3. ANOVA for the quadratic model surface

Source	F-value	p-value	
Model	49.96	< 0.0001	significant
A-Contact time	235.33	< 0.0001	
B-Concentration	85.99	< 0.0001	
C-Temperature	51.64	0.0002	
AB	9.86	0.0164	
AC	0.0814	0.7836	
BC	0.9215	0.3691	
A^2	51.64	0.0002	
B^2	30.59	0.0009	
C^2	3.19	0.1174	

R^2 = 0.9847, Adeq precision = 22.44

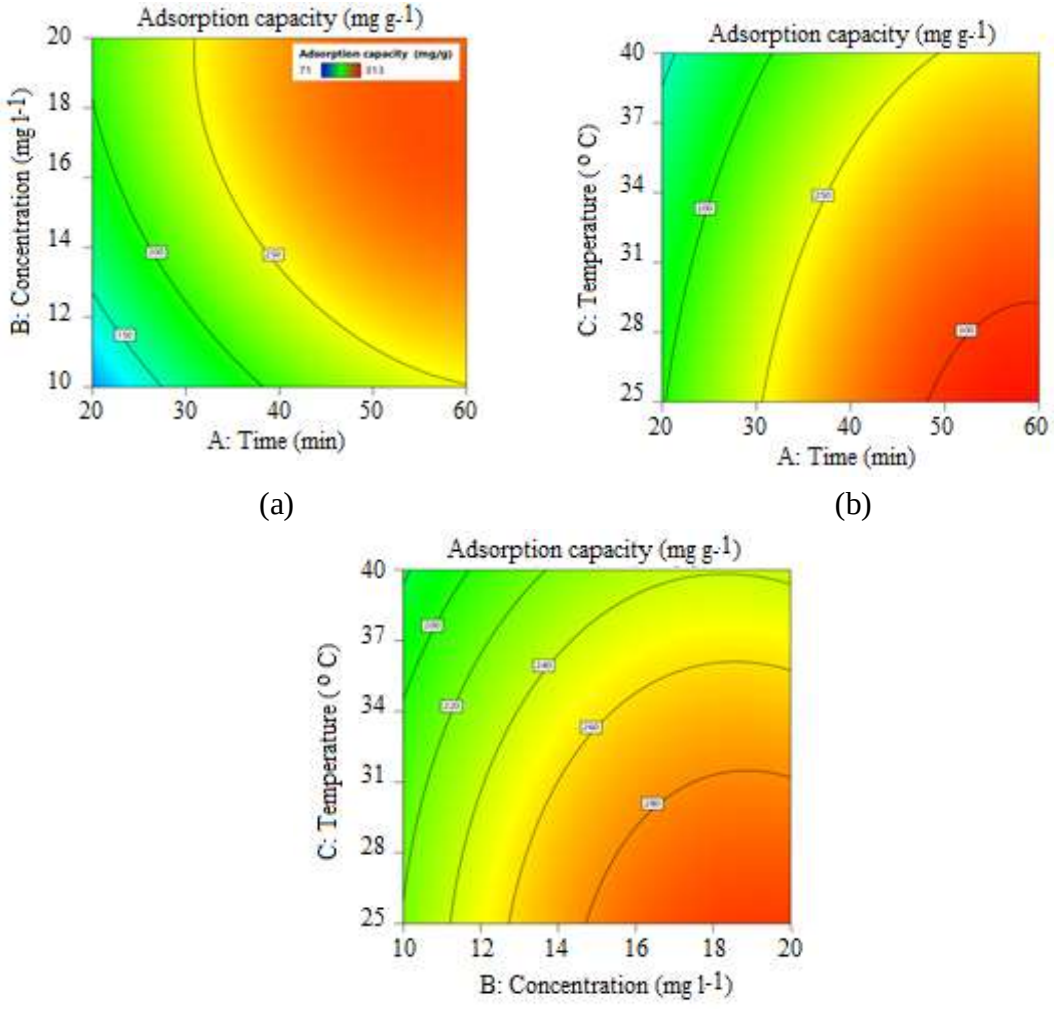

Figure 5. Interactive effects of contact time and initial toluene concentration (a), contact time and temperature (b), initial toluene concentration and temperature (c) on the adsorption capacity of toluene by the magnetic Fe_3O_4/AC.

DOI: http://dx.doi.org/10.32571/ijct.755732 **E-ISSN: 2602-277X**

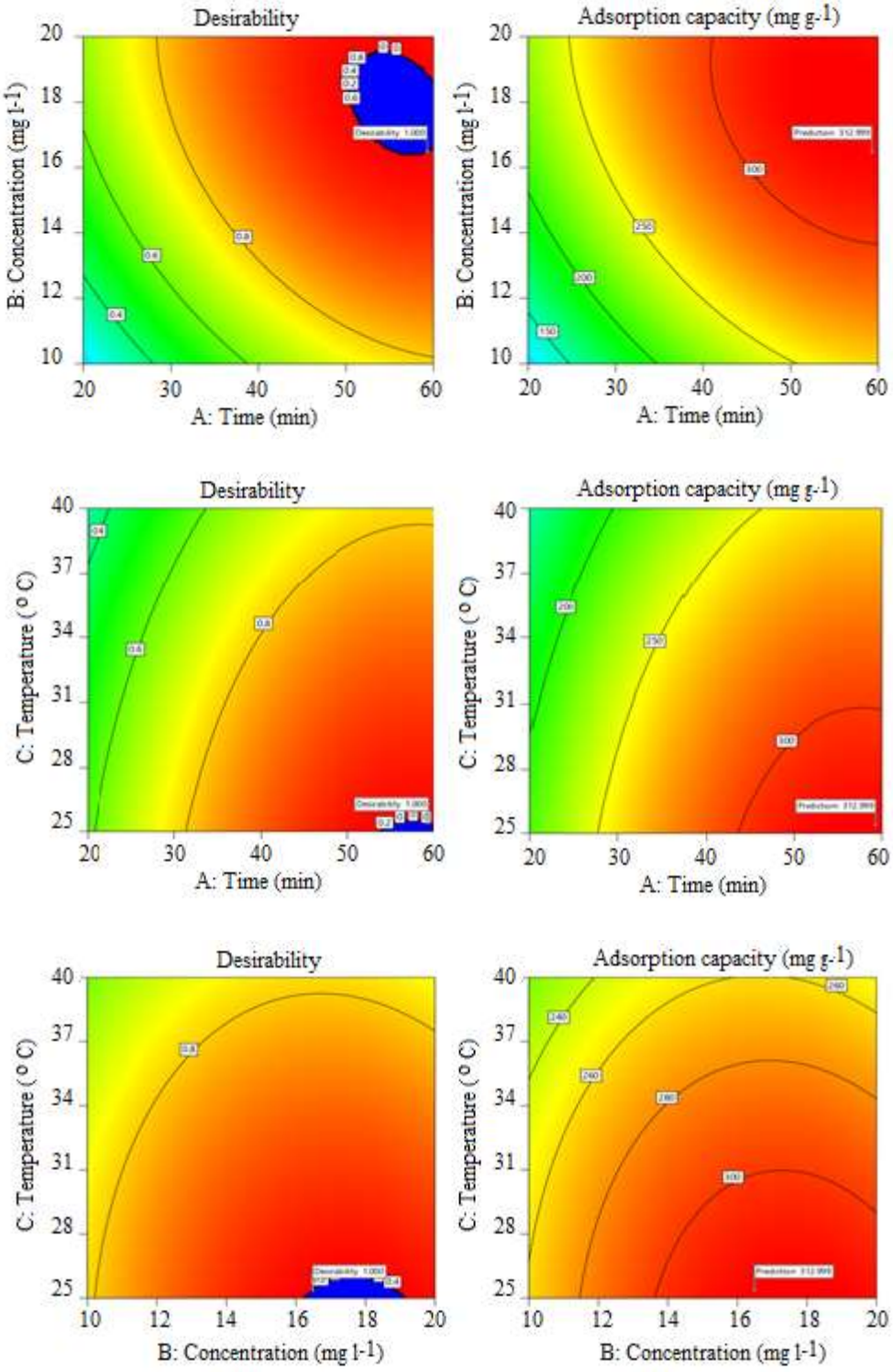

Figure 6. Optimum adsorption conditions of toluene by the magnetic Fe_3O_4/AC.

DOI: http://dx.doi.org/10.32571/ijct.755732 E-ISSN: 2602-277X

3.3. Adsorption kinetics

Under the conditions defined by RSM optimization, pseudo-first-order (PFO) and pseudo-second-order (PSO) kinetic models were used to determine the process mechanism and potential speed control steps in the adsorption of toluene by the magnetic Fe_3O_4/AC. PFO model defines the adsorption rate proportional to the number of empty sites.[18] The non-linear form of the PFO kinetic model is presented with Eq. (2):

$$q_t = q_e(1 - e^{-k_1 t}) \quad (2)$$

Where, q_e and q_t (mg g^{-1}) indicate the amounts of adsorbent adsorbed at equilibrium and any t time (min), respectively. k_1 (1/min) represents the rate constant of the PFO model. This equation is valid for gas/solid adsorption depending on the adsorbent's capacity. It assumes that the change rate in adsorbate absorption over time is proportional to the difference in time and the saturation concentration and adsorbent amount.

The PSO equation, based on the capacity of the adsorption equilibrium, suggests that the fill rate of the adsorption areas is proportional to the square of the number of empty areas. The rate of adsorption is related to the concentration of active sites on the surface of the adsorbent.[18] The non-linear form of the PSO kinetic model is given with Eq. (3) below:

$$q_t = \frac{k_2\, q_e^2\, t}{1 + k_2\, q_e\, t} \quad (3)$$

Where, q_e (mg g^{-1}) is the adsorption capacity at equilibrium, k_2 (g mg^{-1} min^{-1}) is the rate constant of the PSO model. It was determined that the PSO model better defined the adsorption kinetic data for toluene (Figure 7 and Table 4).

Table 4. Adsorption kinetic parameters of toluene by the magnetic Fe_3O_4/AC.

Kinetic models	Parameters	Values
PFO	q_e (mg g^{-1})	317.287
	k_1 (1/min)	0.0584
	R^2	0.985
PSO	q_e (mg g^{-1})	331.675
	k_2 (g mg^{-1} min^{-1})	0.0006
	R^2	0.992

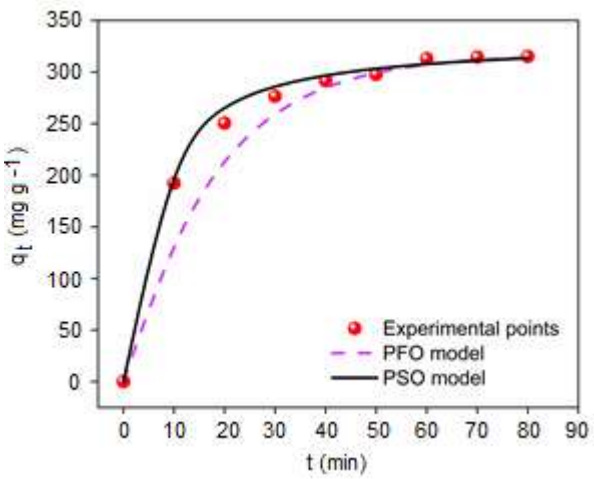

Figure 7. Adsorption kinetics of toluene by the magnetic Fe_3O_4/AC.

3.4. Adsorption isotherms

Under the conditions determined by RSM optimization, Langmuir, Freundlich, and Dubinin-Radushkevich (D-R) models were used to evaluate the equilibrium isotherms for the adsorption of toluene by the magnetic Fe_3O_4/AC.

The Langmuir adsorption isotherm applies to single-layer surface adsorption, including a limited number of identical regions. This model assumes that the adsorption energies on the surface are the same and that there is no adsorbate migration from the surface. Based on these assumptions, the Langmuir model is formulated in the following equation.[19]

$$q_e = \frac{q_{max}\, K_L\, C_e}{1 + K_L\, C_e} \quad (4)$$

Where, C_e (mg l^{-1}) is the equilibrium concentration of the adsorbate, q_e (mg g^{-1}) is the adsorption capacity at equilibrium, q_{max} (mg g^{-1}) is the maximum monolayer adsorption capacity. K_L (l mg^{-1}) is Langmuir isotherm constant.

The main characteristic of the Langmuir isotherm is that the equilibrium parameter, which is a dimensionless constant called the separation factor or equilibrium parameter, can be expressed as R_L:[19]

$$R_L = \frac{1}{1 + K_L C_{in}} \quad (5)$$

In this equation, C_{in} (mg l^{-1}) is the initial concentration.

DOI: http://dx.doi.org/10.32571/ijct.755732 **E-ISSN: 2602-277X**

K_L is the constant related to adsorption energy. R_L value indicates the inconvenience of adsorption nature if R_L is > 1. If R_L = 1, it is linear. If $0 < R_L < 1$, it is suitable.[19] The Freundlich adsorption isotherm is often used to describe the adsorption properties of a heterogeneous surface. This isotherm is formulated with the empirical equation proposed by Freundlich:[19]

$$q_e = K_F C_e^{\frac{1}{n}} \quad (6)$$

In this equation, K_F [(mg g^{-1}) (l $mg^{-1})^{1/n}$] is the Freundlich isotherm constant. n is the adsorption density. C_e (mg l^{-1}) is the equilibrium concentration of adsorbate. q_e (mg g^{-1}) is the adsorption capacity at equilibrium. *1/n* is a function of adsorption power in the adsorption process. The smaller 1/n, the higher expected heterogeneity. This expression is reduced to the linear adsorption isotherm in the situation where *1/n* is 1. If n is between 1 and 10, this situation indicates a suitable adsorption process.[19]

The D-R isotherm model was developed to describe the effect of the porous structure of adsorbent. It is based on the theory of the adsorption potential and suggests that in contrast to the layered adsorption on pore walls, the adsorption process is associated with the filling of the microporous volume. It is argued that the model of the D-R isotherm is superior to the Langmuir isotherm because the Langmuir isotherm takes into account a homogeneous surface or a constant adsorption potential. The non-linear form of this model is described by Eq. (7).

$$q_e = q_s \, exp(-\beta\varepsilon^2) \quad (7)$$

In this equation, q_e (mg g^{-1}) is the adsorption capacity at equilibrium. q_s (mg g^{-1}) is theoretical isotherm saturation capacity. β (mol^2 $(kJ)^{-1}$) is the adsorption energy, and ε (J mol^{-1}) is the adsorption potential. The adsorption potential is described by Eq. (8).[20]

$$\varepsilon = RTln\left(1 + \frac{1}{C_e}\right) \quad (8)$$

In this equation, R (8.314 J mol^{-1} K^{-1}), T (K), and C_e (mg l^{-1}) represent gas constant, absolute temperature, and adsorbate equilibrium concentration, respectively. Adsorption energy is is expressed by Eq. (9).

$$E = \frac{1}{\sqrt{2\beta}} \quad (9)$$

Numerical value of E provides about the adsorption mechanism. If E < 8 kJ mol^{-1}, physical adsorption is dominant. However, in the situation indicating 8 kJ mol^{-1} < E < 16 kJ mol^{-1} and E > 16 kJ mol^{-1}, adsorption occurs by ion exchange and diffusion, respectively.[21]

According to the isotherm data calculated in Table 5, R_L was 0.362, indicating that the Langmuir isotherm model was suitable. In this study, the maximum monolayer adsorption capacity (q_{max}) obtained from the Langmuir isotherm model was 385.208 mg g^{-1}, K_L (Langmuir Constant) was 0.200 l mg^{-1}. The value of R^2 was 0.999, indicating that experimental data was better defined by Langmuir isotherm model in the adsorption of toluene by the magnetic Fe_3O_4/AC. The E value in this study was determined to be 0.446 kJ mol^{-1}, indicating that the adsorption wasa physical process (Figure 8 and Table 5).

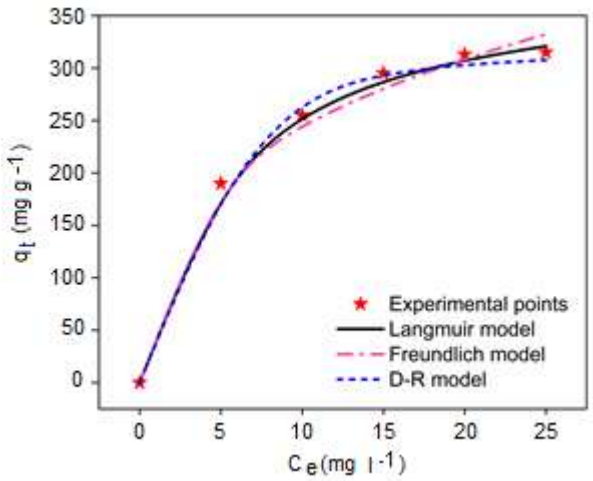

Figure 8. Adsorption isotherms of toluene by the magnetic Fe_3O_4/AC.

Table 5. Adsorption isotherm parameters of tolüene by the magnetic Fe_3O_4/AC.

Isotherm models	Parameters	Values
Langmuir	q_{max} (mg g^{-1})	385.208
	K_L (l mg^{-1})	0.200
	R_L	0.362
	R^2	0.999
Fruendlich	K_F [(mg g^{-1}) (l $mg^{-1})^{1/n}$]	116.396
	n	3.067
	R^2	0.996
D-R	q_s (mg g^{-1})	315.135
	β (mol^2 $(kJ)^{-1}$)	$2.507*10^{-6}$
	E (kJ $mol^{-1)}$	0.446
	R^2	0.997

DOI: http://dx.doi.org/10.32571/ijct.755732 **E-ISSN: 2602-277X**

4. CONCLUSIONS

In this study, we presented the first application of magnetic Fe_3O_4 functionalized with AC as nano-adsorbent for the removal of gas-phase toluene by adsorption process. Firstly, the magnetic Fe_3O_4/AC was synthesized via co-precipitation method within the framework of nanotechnology principles. Then, the effects of process conditions such as contact time, initial toluene concentration, and temperature on the adsorption of toluene by the magnetic Fe_3O_4/AC were investigated using the RSM. The obtained magnetic Fe_3O_4/AC was characterized using SEM, FTIR, and TG analysis. The maximum adsorption capacity for the toluene by the magnetic Fe_3O_4/AC was determined as 312.99 mg g^{-1} under optimal process conditions such as 59.48 min contact time, 17.21 mg l^{-1} initial toluene concentration, and 26.01°C temperature. The adsorption was in the best fit with the Langmuir isotherm model. The adsorption followed by the PSO kinetic model. This study indicated that magnetic Fe_3O_4/AC could be applied as a promising adsorbent for the removal of gas-phase toluene.

ACKNOWLEDGEMENTS

The authors are grateful to the Mardin Artuklu University Research Fund (MAUBAP, Project No. MAÜ.BAP.18.SHMYO.030) for their financial support.

Conflict of interests

Authors declare that there is no a conflict of interest with any person, institute, company, etc.

REFERENCES

1. Kumar, M.; Giri, B. S.; Kim, K.-H.; Singh, R. P.; Rene, E. R.; López, M. E.; Rai, B. N.; Singh, H.; Prasad, D.; Singh, R. S. *Bioresour. Technol.* **2019,** 285, 121317.

2. Kutluay, S.; Baytar, O.; Şahin, Ö. *Res. Eng. Struct. Mater.* **2019,** 5 (3), 279-298.

3. Ryu, H. W.; Song, M. Y.; Park, J. S.; Kim, J. M.; Jung, S. C.; Song, J.; Kim, B. J.; Park, Y. K. *Environ. Res.* **2019,** 172, 649-657.

4. Xu, P.; Wei, Y.; Cheng, N.; Li, S.; Li, W.; Guo, T.; Wang, X. *J. Hazard. Mater.* **2019,** 366, 105-113.

5. Temel, F.; Kutluay, S. *New J. Chem.* **2020,** 44 (30), 12949-12961.

6. Temel, F.; Tabakci, M. *Talanta* **2016,** 153, 221-227.

7. Şahin, Ö.; Saka, C.; Kutluay, S. *J. Ind. Eng. Chem.* **2013,** 19 (5), 1617-1623.

8. Saka, C.; Şahin, Ö.; Kutluay, S. *Energ. Source. Part A* **2016,** 38 (3), 339-346.

9. Tor, A.; Aydin, M. E.; Aydin, S.; Tabakci, M.; Beduk, F. *J. Hazard. Mater.* **2013,** 262, 656-663.

10. Connie, Z. Y.; Ariya, P. A. *Int. J. Environ. Sci.* **2015,** 31, 164-174.

11. Bhatia, D.; Datta, D.; Joshi, A.; Gupta, S.; Gote, Y. *J. Chem. Eng.* **2018,** 63 (2), 436-445.

12. Kutluay, S.; Baytar, O.; Şahin, Ö. *J. Environ. Chem. Eng.* **2019,** 7 (2), 102947.

13. Zhao, Z.; Wang, S.; Yang, Y.; Li, X.; Li, J.; Li, Z. *Chem. Eng. J.* **2015,** 259, 79-89.

14. Juang, R. S.; Yei, Y. C.; Liao, C. S.; Lin, K. S.; Lu, H. C.; Wang, S. F.; Sun, A. C. *J. Taiwan. Inst. Chem. Eng.* **2018,** 90, 51-60.

15. Kutluay, S.; Baytar, O.; Şahin, Ö.; Arran, A. *Eur. J. Tech.* **2020,** 10 (1), 131-142.

16. Baytar, O.; Şahin, Ö.; Horoz, S.; Kutluay, S. *Environ. Sci. Pollut. Res.* **2020**, 27, 26191–26210.

17. Vohra, M. S. *Arab. J. Sci. Eng.* **2015,** 40 (11), 3007-3017.

18. Ali, R. M.; Hamad, H. A.; Hussein, M. M.; Malash, G. F. *Ecol. Eng.* **2016,** 91, 317-332.

19. Dada, A.; Olalekan, A.; Olatunya, A.; Dada, O. *IOSR J. Appl. Chem.* **2012,** 3 (1), 38-45.

20. Hu, Q.; Zhang, Z. *J. Mol. Liq.* **2019,** 277, 646-648.

21. Sadeghalvad, B.; Azadmehr, A.; Hezarkhani, A. *RSC Adv.* **2016,** 6 (72), 67630-67642.